BOLETIN DE LA SOCIEDAD ESPAÑOLA DE
Cerámica y Vidrio
www.elsevier.es/bsecv

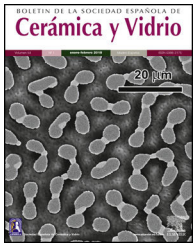

Original

Effect of temperature and clay addition on the thermal behavior of phosphate sludge

Mohamed Amine Harech[a,*], *Mohamed Mesnaoui*[a], *Younes Abouliatim*[b], *Youssef EL hafiane*[c], *Abdelaziz Benhammou*[b], *Abdelkrim Abourriche*[b], *Agnes Smith*[c], *Lahbib Nibou*[b]

[a] *Laboratoire Sciences des Matériaux Inorganiques et leurs applications: Equipe Chimie de la Matière Condensée et de l'Environnement, ECMCE, FSSM, Université Cadi Ayyad, Maroc*
[b] *Laboratoire Matériaux Procédés Environnement Qualité, LMPEQ, ENSA de Safi, Université Cadi Ayyad, Maroc*
[c] *Institut de recherche sur les céramiques, IRCER - UMR 7315, Université de Limoges, Centre Européen de la Céramique, 12 rue Atlantis, 87068 Limoges Cedex, France*

ARTICLE INFO

Article history:
Received 5 October 2019
Accepted 3 March 2020

Keywords:
Phosphate sludge
Safi clay
Thermal treatment
Mineralogical transformations

ABSTRACT

The aim of the present work is to characterize the phosphate sludge from the area of Youssoufia (rich in CaO ~ 31%) and to study its thermal behavior alone and when mixed with clay from Safi (Morocco). This may contribute to its valorization as an alternative raw material for ceramic industries. The evolution of phases during the thermal treatment of phosphate sludge, clay and sludge–clay mixtures at different mass ratios (25 wt%, 50 wt%, and 75 wt%) was performed at different levels of temperatures from 600 to 1120 °C. Mineralogical analysis by X-ray diffraction (XRD) showed that the sludge mainly consisted of quartz, calcite, dolomite, and francolite. Dolomite and calcite vanished after sludge heating and two new phases were formed, namely akermanite and monticellite. For clay, it mainly consisted of illite, kaolinite, quartz, calcite, and dolomite. After clay sintering at high temperature, a new phase was formed, i.e. anorthite. The effects of the MO/SiO_2 ratio (MO = CaO + MgO) in mixtures (clay + sludge) on the crystallization behavior of diopside and fluorapatite, and the disappearance of the akermanite were investigated. The results showed that the crystallization of diopside–fluorapatite increased when the MO/SiO_2 ratio increased.

Efecto de la temperatura y la adición de arcilla sobre el comportamiento térmico del lodo de fosfato

Palabras clave:
Lodos de fosfato

RESUMEN

El objetivo del presente trabajo es caracterizar un lodo de fosfato del área de Youssoufia (rico en CaO ~ 31%) y estudiar su comportamiento térmico tras su mezcla con una arcilla de Safi

* *Corresponding author.*
E-mail address: mharech@gmail.com (M.A. Harech).
https://doi.org/10.1016/j.bsecv.2020.03.002

Arcilla de Safi
Tratamiento térmico
Transformaciones mineralógicas

(Marruecos). Este estudio puede contribuir a su valorización como materia prima alternativa para la industria cerámica. La evolución de las fases minerales durante el tratamiento térmico de lodos de fosfato, arcilla y mezclas de lodos y arcilla en diferentes proporciones de masa (25, 50 y 75% de peso) se realizó a diferentes temperaturas, desde 600 a 1.120 °C. El análisis por difracción de rayos X (DRX) permitió conocer la composición mineralógica del lodo formado principalmente por cuarzo, calcita, dolomita y francolita. La dolomita y la calcita desaparecieron tras el calentamiento del lodo y se formaron 2 nuevas fases, a saber, akermanita y monticellita. En cuanto a la arcilla, el análisis mineralógico evideció la presencia de illita, caolinita, cuarzo, calcita y dolomita como fases mayoritarias. Tras la descomposicón de la arcilla se formó anortita como fase de alta temperatura. Se investigaron los efectos de la relación MO/SiO_2 (MO = CaO + MgO) en mezclas (arcilla + lodo) sobre la cristalización de diópsido y fluorapatita y la desaparición de la akermanita. Los resultados mostraron que la cristalización de diopsido-fluorapatita aumentó cuando creció el cociente MO/SiO_2.

Introduction

Morocco possesses around three-quarters of the world's phosphate reserves and is the third largest producer of phosphate [1]. It is the leading exporter of phosphate and its derivatives. This Industry is carried out by a combination of successive mineral processing steps involving crushing, screening, washing, and flotation, generating a huge amount of phosphate sludge that was estimated in 2010 to about 28.1 million tons [2]. This sludge is deposited in large surface ponds. As proven by recent research, the phosphate sludge is not polluting surface nor underground water [3,4]. However, the physical changes in the environment, as well as the huge footprints of the mine site areas, are the main environmental implication of the phosphate sludge [2]. During the last decade, the potential valorization of phosphate mine by-products has become a question of great importance [1,2,5,6].

Several authors have investigated the valorization of the sludge outcome of the phosphate washing process in the area of Youssoufia (Morocco). Loutou et al. carried out several studies to valorize the phosphate sludge through the elaboration of light aggregate [1]. Other studies investigated the microstructure of expandable lightweight aggregates of clay, cement and phosphate waste and evaluated the release of phosphorus and their effect on the growth of alfalfa plants [7]. Recently, Moukannaa et al. studied the use of phosphate mine tailings for the production of geopolymers [5]. The findings indicate that phosphate sludge from Youssoufia consists of quartz, calcite, dolomite, and fluorapatite.

Morocco has become known all across North Africa and Europe for its pottery and ceramics. Fes-Meknes, Sale and especially Safi are the main pottery centers of the country, producing about eighty percent of Morocco's production. Exploitation of clay minerals in Safi is mainly artisanal and semi-industrial, by family firms and more than 500 artisans. Clay minerals reserves in Safi are sufficient to satisfy the demand of the ceramic industry. However, in order to protect non-renewable natural resources we study the feasibility to incorporate the industrial phosphate sludge come from Youssoufia to reduce the rate of clay use. In this work we have chosen phosphate sludge for its important annual production and also for the geographical proximity between Safi ceramic companies and the location of this waste: these two cities are less than an hour apart. This makes it possible to use phosphate sludge as raw material of ceramic industry developed by the factories in Safi.

Safi clay, which consists of clay phases and ancillary minerals, is largely used for artisanal ceramic manufacturing because of its good plasticity. It is considered as a source of alkalis, silicate, and alumina. These oxides, react at high temperatures and may induce vitreous and refractory phases [8].

The aim of this work is to understand the evolution of phases during the thermal treatment and appreciate the effect of the clay addition on the sludge phase's transformations. What is new about this study is the sharp focus on the chemical transformation of clay–sludge mixture (25, 50, 75 wt% clay), to trace the evolution of the phases formed at low and medium temperatures (900–1120 °C), and to find to what extent these mixtures could be applied to the predefined phases.

Materials and methods

Raw materials preparation

Raw materials used in this study were red clay obtained from "AL BARRAGE" (a region in Safi, Morocco with a coordinates 32.324962, -9.188877) and phosphate sludge collected from the Youssofia industrial phosphate wash plant. Initially, both raw materials were dried at 105 °C for 5 h in an electrical oven, then they were crushed and sieved using a 100-μm sieve.

Samples elaboration

Five mixtures, M1–M5, were prepared with the mass proportions, in clay/phosphate sludge, as follows: M1: 1/0, M2: 0.75/0.25, M3: 0.5/0.5, M4: 0.25/0.75 and M5: 0/1. Table 1 shows the mass proportions of mixtures.

The pellets were prepared by dry process from raw material powders, homogeneously mixed by a co-grinding of both powders. The mixed powder was axially compressed under a

Table 1 – Percentage of clay–sludge mixtures.

	M1	M2	M3	M4	M5
Clay	100%	75%	50%	25%	0%
Sludge	0%	25%	50%	75%	100%

one-ton charge to get pellets with 13 mm diameter and 3 mm thickness, which were then heated at different temperatures. The firing cycle was the following: i. heating ramp 5 °C/min up to the selected firing temperature (600, 900, 1000, 1100, and 1120 °C); ii. 2 h dwell time at the temperature selected; iii. cooling according to the inertia of the furnace. The heat treatments were carried out in an electric furnace (Nabertherm model LH 15/12). Fig. 1 shows the the sample preparation process.

Characterization techniques

The chemical composition of clay and phosphate sludge was determined by using Panalytical ZETIUM X-ray fluorescence (XRF) analysis. An ICP-AES instrument perkinElmer Optima 8300 DV was used for the simultaneous multielement determination of major and minor elements. Sample preparation for ICP-AES analysis was performed: 20 mg of sludge and clay samples were accurately weighed into Teflon digestion vessels, and 4 ml of a concentrated HF solution with 1 ml of a HNO_3 solution were added. Samples were subjected to the microwave heating for 75 min. After cooling, colorless solutions were quantitatively transferred into 100 ml volumetric flasks and made up to the volume with deionised water. The mineralogical characterization of the crystalline phases formed after thermal treatment were performed by X-ray diffraction using a Bruker D8 Advance diffractometer, operating with Cu Kα radiation, an operating voltage of 40 kV, a current of 40 mA, a step size of 0.02° and a scanning angle 2θ ranging from 5° to 60°. The presence of minerals was identified from the position of peaks and its intensities were matched by using reference database from software and X'Pert HighScore. The enhancement or inhibition of a certain crystalline phase was mainly judged from the presence or absence of its specific diffraction lines and the increase or decrease in their relative intensities..

The heat flow and weight loss of the clay and sludge were tracked as a function of the temperature using the coupled TG-DTA (thermal gravimetric-differential thermal analysis). The unfired powders were analyzed with a Setaram 92 instrument. Data were collected under air from 30 to 1000 °C at a heating rate of 10 °C/min.

Results and discussion

Thermal behavior of phosphate sludge

Table 2 lists the chemical composition of raw materials. It can be seen that the phosphate sludge is mainly composed of CaO 31.44 wt%, SiO_2 27.48 wt% and P_2O_5 16.83 wt%, with a small quantity of MgO and Al_2O_3 (respectively 2.90–2.41 wt%). The elemental analyses of phosphate sludge (Table 3) were used to quantify the major and minor elements and also heavy metals and radionuclides. From the results of the analysis of the samples, phosphorus was found to be 13.52 mg/l, silicon was 23.7 mg/l, and calcium was 41.46 mg/l, also, minor elements were detected (aluminum, iron, potassium, and titanium). There was no heavy metals and radionuclides present. The X-ray diffractogram of the sludge shown in Fig. 2 revealed the following mineralogical composition: quartz (SiO_2), calcite ($CaCO_3$), dolomite ($CaMg(CO_3)_2$) and francolite $Ca_{5+0.5x}(PO4)_{3-x}(CO3)_x(F,OH)$.

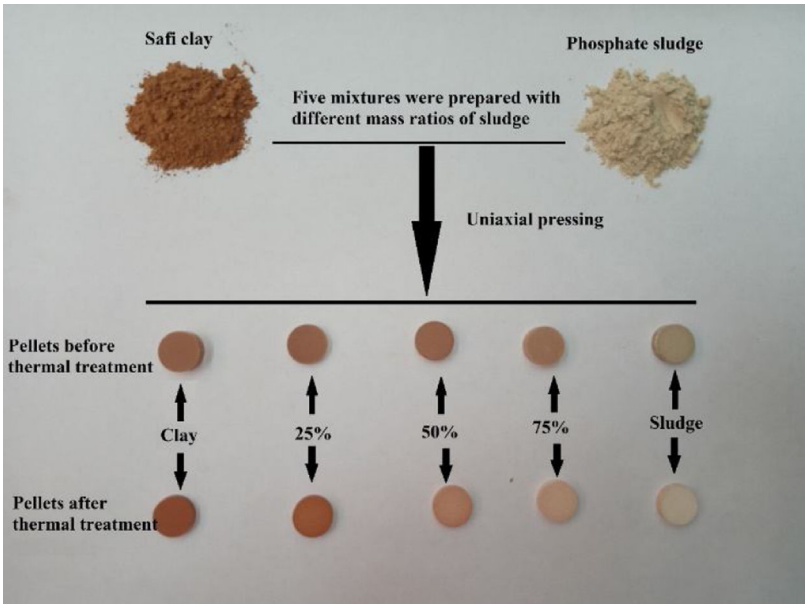

Fig. 1 – Illustrated synthesized process of ceramics samples.

Table 2 – Chemical composition of sludge and clay (wt%).

	CaO	SiO_2	P_2O_5	MgO	Al_2O_3	SO_3	Fe_2O_3	K_2O	Na_2O	TiO_2	LOI
Sludge	31.44	27.48	16.83	2.90	2.41	1.26	0.93	0.42	0.30	0.19	15.64
Clay	3.94	52.79	0.17	2.53	17.44	Bdl*	5.85	4.62	0.42	Bdl*	11.7

* Bdl: below detection limit.

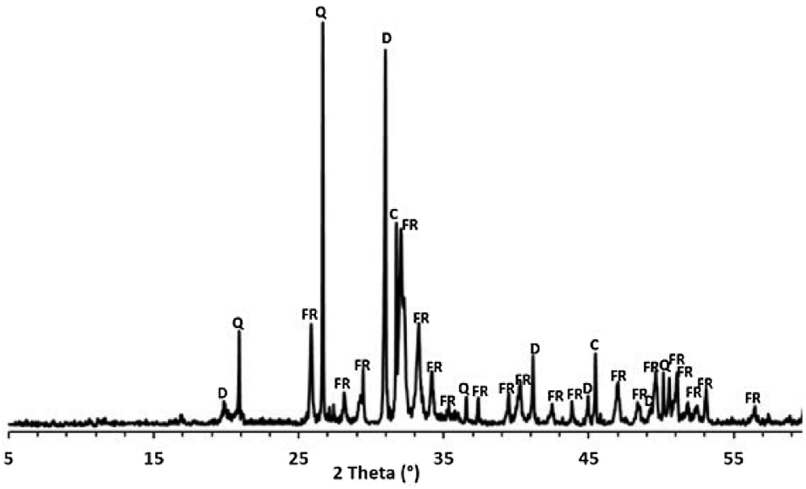

Fig. 2 – XRD diffraction patterns of sludge. Q: quartz; FR: francolite; C: calcite; D: dolomite.

Table 3 – Elemental analysis of phosphate sludge and clay (mg/l).

Analyste name	Clay	Sludge
Al	33.52	2.35
Ca	8.88	41.46
Fe	17.57	1.18
K	14.45	0.65
Mg	3.92	3.23
Na	1.10	0.41
Si	98.30	23.7
Ti	Bdl*	0.2
P	0.26	13.52
S	Bdl*	0.93
Cd	Bdl*	Bdl*
Pb	Bdl*	Bdl*

* Bdl: below detection limit.

Francolite and fluorapatite are two phases presenting almost the same diffractogram, the only difference is at the level of the peaks between 30 and 35 2theta, francolite presents three peaks and fluorapatite presents four peaks. Fig. 3 illustrates the difference between the theoretical diffractogram of francolite and fluorapatite. Many studies have demonstrated that fluorapatite $Ca_5(PO_4)_3F$ is the major phase in the Yousoufia sludge [1,2,5,6]. However, the results of the present study showed the absence of the fluorapatite while the francolite is the major phase contained in this sludge. Francolite which is a carbonate fluorapatite with the common formula of $Ca_{5+05x}(PO4)_{3-x}(CO3)_x(F,OH)_{(s)}$, appears when the PO_4^{3-} within the structure of fluorapatite is substituted by CO_3^{2-}. CO_3^{2-} content of francolites vary from 1.4% to 6.3% [12,13]. The maximum level of carbonate substitution is limited by the disruption of the francolite structure at high contents of CO_2 (>6.3%). Many studies have shown that PO_4^{3-} is replaced by ($CO_3^{2-} + F^-$) and not by CO_3^{2-} alone [9,10]. Other studies have reported that PO_4^{3-} and Ca^{2+} are replaced by CO_3^{2-} [11].

The value of LOI 15.64 wt% for sludge is due to the content of carbonate, dehydroxylation and water release.

The phase evolution of phosphate sludge during heat treatment was studied by XRD analysis. Fig. 4 shows the XRD patterns of phosphate sludge powder after sintering at 600, 900, 1000, 1100 and 1120 °C.

After the first heating at 600 °C dolomite decomposes to $CaCO_3$ and $MgCO_3$. However, at 900 °C, calcite is not detected and the francolite phase transformed into fluorapatite $Ca_5(PO_4)_3F$. At 900 °C, a few major changes can be seen, including calcite phase disappearance and the decrease in quartz peaks intensity as well as the increase in the intensity of two new phases akermanite and monticelitte. The weakening of SiO_2 and disappearance of $CaCO_3$ peaks at 900 °C is due to the monticelitte formation according to the reaction shown in Table 4. Monticelitte $CaMgSiO_4$ is considered intermediate compounds, which became unstable at high temperatures and react with SiO_2 and CaO to give akermanite ($Ca_2MgSi_2O_7$). Above 1000 °C, the major phases found are the fluorapatite, akermanite and quartz [14,15].

To confirm the presence of francolite and how it transforms into fluorapatite, a zoom in the region between $2\theta = 30–35°$ was placed in Fig. 4. The diffractogram corresponding to this area is shown in Fig. 5. The three peaks of francolite phases in $2\theta = 30–35°$ change their position and display a doublet characteristic of fluorapatite phase before 900 °C.

The thermal behavior of the sludge analyzed by TG-DTA is presented in Fig. 6. Five endothermic peaks are clearly shown

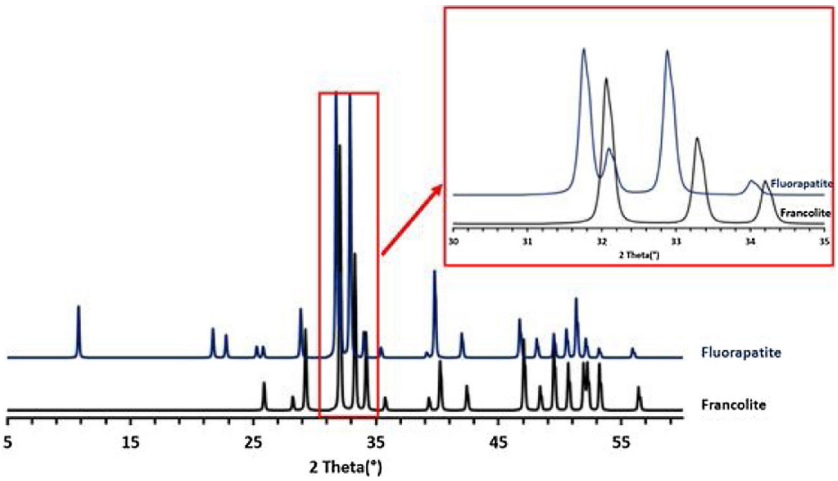

Fig. 3 – Theoretical XRD patterns of francolite and fluorapatite phases.

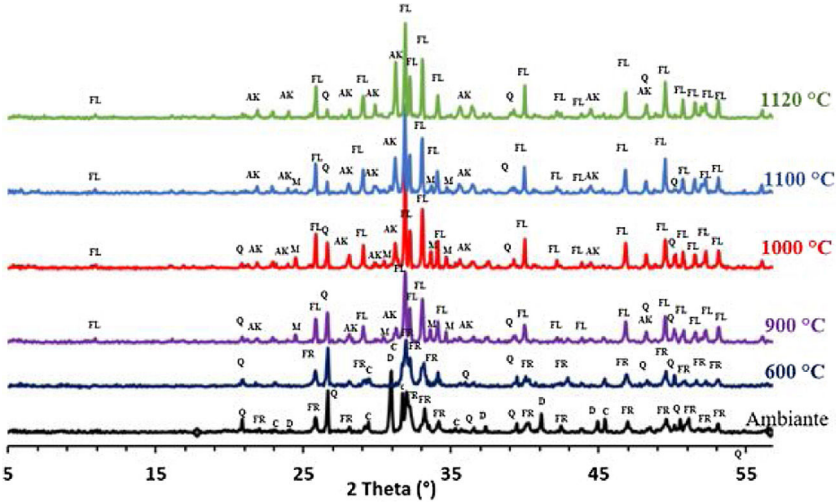

Fig. 4 – XRD patterns of sludge sintered at different temperatures. Q: quartz; C: calcite; D: dolomite; FR: francolite; FL: fluorapatite; AK: akermanite.

in the DTA curve; the first peak at 93 °C is probably attributed to the removal of weakly bound water. The endothermic peak detected at 575 °C could be assigned to the decomposition of dolomite. No discernable mass loss was observed by the TGA curves at the same temperature, while the peak shown at 700 °C is corresponding to the transformation of francolite to fluorapatite. Peaks at 736 and 746 °C could be attributed to the decomposition of calcite and magnesium carbonate, respectively. TGA curve indicated that these changes were responsible for the mass loss.

To confirm the above transformations and for understanding better the reactions that occurred during the thermal treatment, calcination has been carried out at three additional temperatures: 720 °C, 750 °C and 800 °C. The results of the XRD analysis in the region $2\theta = 28–35°$ are presented on the diffractogram in Fig. 7. They show the presence of francolite and calcite where their peaks are detected at 600 °C. At 720 °C we notice the appearance of fluoroapatite and the disappearance of francolite, which occurred between 600 and 720 °C. XRD diffraction patterns of sludge sintered at 750 °C revealed the missing of calcite. The results of the XRD analyses are in good agreement with the findings from the DTA, which confirms that the transformation of francolite to fluoroapatite and the decomposition of calcite are occurring at around 700 and 746 °C respectively.

Thermal behavior of Safi clay

Chemical analysis (Table 2) shows that Safi clay is essentially composed of SiO_2 (52.79 wt%), Al_2O_3 (1744 wt%), Fe_2O_3 (5.85 wt%). Besides, there are a little amount of other oxides such as Na_2O, MgO, and P_2O_5. Table 3 lists the elemental analysis of raw materials. It can be seen that the clay is mainly composed of silicon 98.30 mg/l, aluminum 35.52 mg/l, iron 17.57 mg/l and potassium 14.45 mg/l with a small quantity of phosphorus and sodium (respectively 0.26–1.10 mg/l). These results are in good agreement with the X-ray fluorescence analyses. The crystalline phase com-

Table 4 – Sludge phases evolution as a function of temperature.

Temperature	Phases	Reaction	Ref
Untreated	Quartz Dolomite Calcite Francolite	no reaction	
30°C-600°C	Quartz Calcite Francolite	$CaMg(CO_3)_{2(s)} \rightarrow CaCO_{3\ (s)} + MgCO_{3(s)}$	[12]
600°C - 900°C	Quartz Fluorapatite Akermanite Monticelitte	$CaCO_{3(s)} \rightarrow CaO_{(s)} + CO_{2\ (g)}$	[13]
		$Ca_{5+0.5x}(PO4)_{3-x}(CO3)_x(F.OH)_{(s)} \rightarrow Ca_5(PO4)_3(F.OH)_{\ (s)} + CO_{2(g)} + CaO_{(s)}$	[11]
		$CaO_{\ (s)} + MgO_{\ (s)} + SiO_{2\ (s)} \rightarrow CaMgSi_2O_{4(s)}$	[14]-[15]
1000°C	Quartz Fluorapatite Akermanite Monticelitte	$CaMgSiO_4 + CaO + SiO_2 \rightarrow Ca_2MgSi_2O_7$	[16]
1100°C	Quartz Fluorapatite Akermanite Monticelitte	No reaction	
1120°C	Quartz Fluorapatite Akermanite	No reaction	

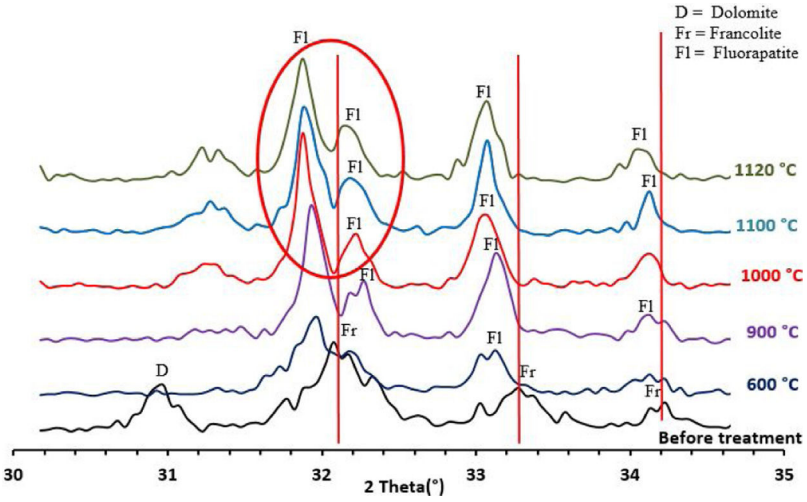

Fig. 5 – Zoom in region of 30–35° XRD patterns of sludge sintered at different temperatures.

position and the phase evolution of clay were obtained by XRD analysis. The main detected minerals (Fig. 8) were illite $K_{0.5}$ $(Al,Fe,Mg)_3(Si,Al)_4O_{10}(OH)_2$, kaolinite $(Al_2Si_2O_5(OH)_4)$, dolomite $(CaMg(CO_3)_2)$, calcite $(CaCO_3)$ and quartz (SiO_2). The value of LOI for clay (11.7 wt%) is due to the content of carbonate, dehydroxylation and water release.

Fig. 9 shows the XRD patterns of clay powder after sintering at 600, 900, 1000, 1100 and 1120 °C, After heating of clay at 600 °C, kaolinite decomposes to amorphous metakaolinite $(Al_2Si_2O_7)$ by removing of the hydroxyl groups of the silicate lattice according to Eq. (1). While dolomite was decomposed to calcite and magnesium carbonate as shown in Eq. (2).

$$Al_2Si_2O_5(OH)_{4(s)} \rightarrow Al_2Si_2O_{7(s)} + 2H_2O_{(g)} \quad (1)$$

$$CaMg(CO_3)_{2(s)} \rightarrow CaCO_{3(s)} + MgCO_{3(s)} \quad (2)$$

As the temperature increased to 900 °C, calcite was decarbonized, the intensity of illite decreased and the peaks in the region $2\theta = 26–29°$ increased in intensity, which indicates the

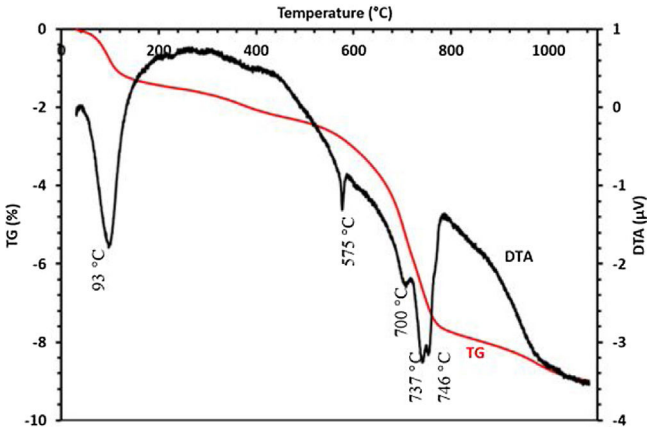

Fig. 6 – TG-DTA analysis of sludge.

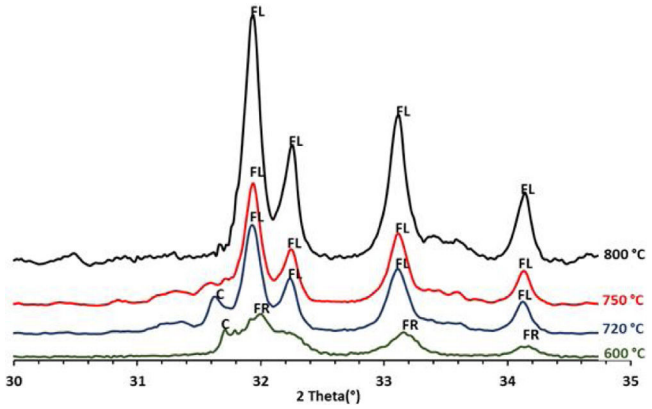

Fig. 7 – Zoom in region of 30–35° XRD patterns of sludge sintered at intermediate temperatures.

formation of anorthite. This may be attributed to the reaction between Metakaolin produced following the dehydroxylation of the kaolinite and CaO produced following the decomposition of the calcite [17,18]. The content of anorthite phase increases as the temperature increases, after 900 °C the free silica reacts with free CaO and alumina, the last being derived from the decomposition of illite, forming anorthite.

As a matter of fact, wollastonite $CaSiO_3$ and gehlenite $Ca_2Al_2SiO_7$ are considered intermediate compounds which became unstable in the presence of SiO_2 and react to give anorthite ($CaAl_2(SiO_4)_2$). However in this study, gehlenite and wollastonite were not detected, this is due to the large SiO_2 content of clay [19,20].

From 1000 °C onwards, remarkable changes were noticed. Accordingly, the traces of a new phase called diopside, start to appear after reaction between three oxides: CaO originated from calcite and dolomite, MgO produced following the decomposition of dolomite and SiO_2 present in the initial composition of the clay. The quartz is present in all the raw and fired samples, with contents decreasing progressively with temperature. Table 5 summarizes all the reactions associated with the thermal treatment of clay as reported in the literature [22,23].

The DTA–TGA thermograms of clay given in Fig. 10 show the major transformation that clay undergoes as a function of temperature. A first weight loss was detected at 95 °C corresponding to the evaporation of free water contents. The dehydroxylation of the kaolinite mineral as a result of the increase in temperature induces a large endothermic peak at 508 °C, which hides the peak corresponding to the decomposition of dolomite. The small peak at 568 °C corresponds to the transformation of quartz α to quartz β, while the peak at 736 °C is attributed to the decomposition of calcite and magnesium carbonate.

Thermal behavior of mixtures

The phase evolution of clay/sludge mixture as a function of the clay addition percentage (25 wt%, 50 wt%, 75 wt%) during heat treatment was studied by XRD analysis. Figs. 11 and 12 show the XRD patterns of mixtures after sintering at 900 and 1120 °C respectively. These temperatures were chosen with a view to study the evolution of the mixture at low temperatures (900 °C) and high temperature (>1100 °C).

The X-ray diffraction analysis, of the pellets sintered at 900 °C, made from the mixture with 25 wt% clay (Fig. 11),

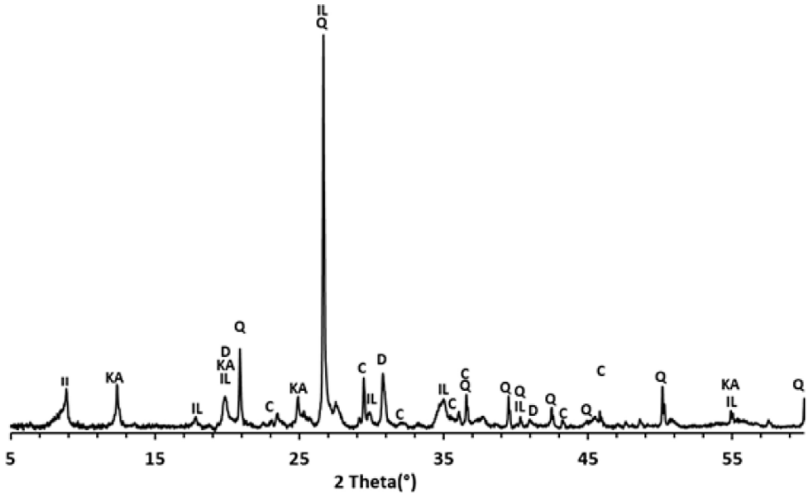

Fig. 8 – XRD diffraction patterns of Safi clay. Q: quartz; C: calcite; D: dolomite; IL: illite; KA: kaolinite.

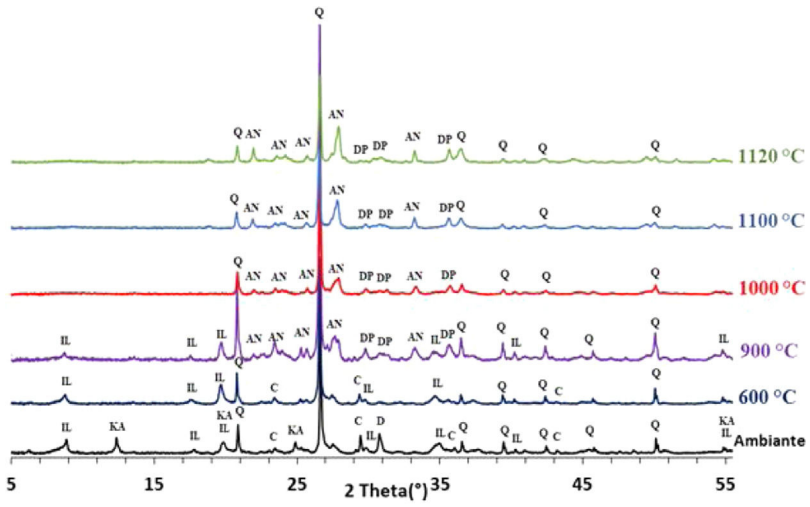

Fig. 9 – XRD patterns of clay sintered at different temperatures. Q: quartz; D: dolomite; IL: illite; KA: kaolinite; AN: anorthite; DP: diopside.

Table 5 – Clay phases evolution as a function of temperature.

Temperature	Phases	Reaction	Ref
Untreated	Quartz Dolomite Calcite Illite Kaolinite	no reaction	
30°C-600°C	Quartz Calcite Illite	$CaMg(CO_3)_{2(s)} \rightarrow CaCO_{3\,(s)} + MgCO_{3(s)}$ $Al_2Si_2O_5(OH)_{4\,(s)} \rightarrow Al_2Si_2O_{7(s)} + 2\,H_2O_{(g)}$	[12] [18]
600°C - 900°C	Quartz Illite Diopside Anorthite	$CaCO_{3(s)} \rightarrow CaO_{(s)} + CO_{2\,(g)}$	[13]
		$CaO_{(s)} + MgO_{(s)} + 2SiO_2(s) \rightarrow CaMg(SiO_3)_{2(s)}$	[21]. [22]
		$CaO_{(s)} + Al_2Si_2O_{7(s)} \rightarrow CaAl_2(SiO_4)_{2(s)}$ $CaO_{(s)} + Al_2O_{3(s)} + 2\,SiO_{2(s)} \rightarrow CaAl_2(SiO_4)_{2(s)}$	[23] [24]
1000°C-1100°C	Quartz Diopside Anorthite	no reaction	
1100°C	Quartz Diopside Anorthite	no reaction	
1120°C	Quartz Diopside Anorthite	no reaction	

revealed the presence of quartz, fluorapatite and traces of anorthite. The akermanite and monticelitte vanished and diopside appeared, these evolutions are discussed hereafter. At the same temperature and for the mixture with 50 wt% clay, diopside and fluorapatite phases increased and become the major phases. Yet, a gradual decrease of quartz and anorthite phases have been noticed. At high percentage of clay, a decrease in the amount of fluorapatite and diopside phases was observed, while the anorthite phase started to be the major phase.

As shown in Fig. 12, increasing the firing temperature to 1120 °C, led a decrease in the amount of quartz and an increase in the diopside within the mixtures 25 wt% and 50 wt% (wt% clay). The formation of the diopside is favored by increasing the firing temperature as well as the high percentage of phosphate sludge. It can be observed that akermanite and monticelitte phases completely disappeared in all mixtures following the formation of the diopside phase.

Akermanite, monticelitte and diopside are three varieties that have simple chemical compositions mainly constituted

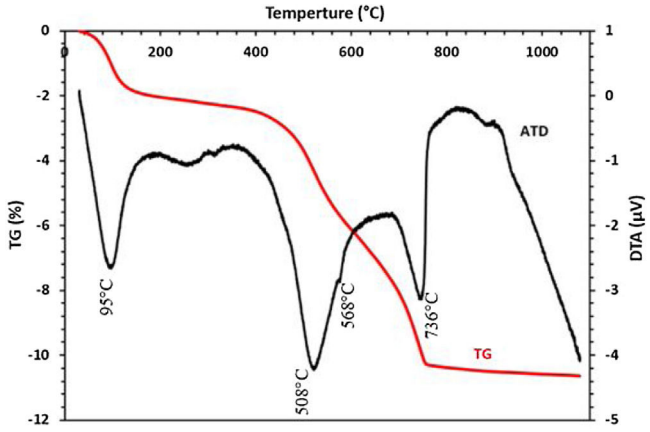

Fig. 10 – TG-DTA analysis of Safi clay.

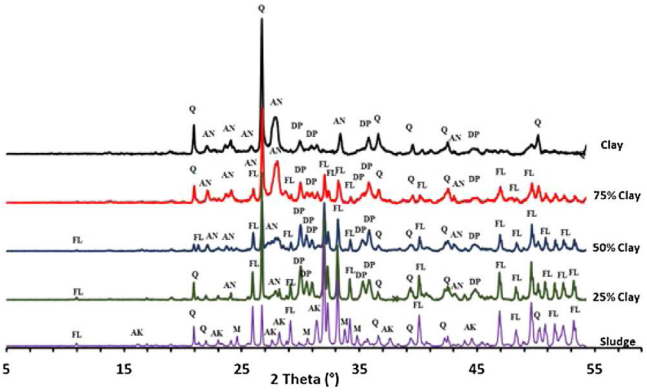

Fig. 12 – XRD patterns of sludge–clay mixtures sintered at 1120 °C.

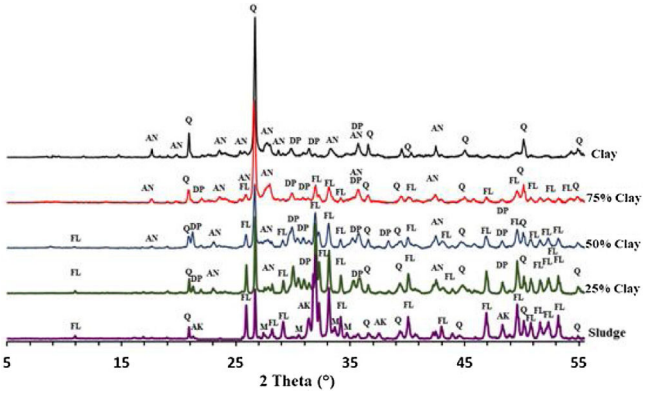

Fig. 11 – XRD patterns of sludge–clay mixtures sintered at 900 °C.

by SiO_2, MgO and CaO [24]. The system CaO–MgO–SiO_2 (Fig. 12) is very useful in providing a framework for the understanding of the equilibrium between akermanite and diopside phases within the sludge–clay mixture [25]. The firing behavior of no-calcareous and calcareous samples is considerably different because of the initial mineralogical composition. Moreover, the presence of dolomite, calcite or both, with a large percentage can influence the formation of different minerals after firing behavior at high temperatures [19].

The competition between the formation of diopside and akermanite during the heating was influenced by the composition and thermodynamic of the system. The above experimental results indicate that the amount of CaO and SiO_2 may play a key role on the formation of diopside phase in the investigated system.

The main difference between the raw materials (clay and sludge) is the composition of the carbonate. As has been shown in the intensities of the most intensive diffraction peaks for the crystalline phases in sludge and clay, calcite and dolomite are lightly present in clay, unlike in sludge.

Another difference is the percentage of quartz, the chemical composition of clay has a higher contribution of SiO_2. The quartz concentration was strongly enhanced during the enrichment of mixtures by clay. So, the addition of clay corresponded to a higher contribution of SiO_2. Hence, the ratio MO/SiO_2 (MO = CaO + MgO) decreased, which indicates that the formation of Metasilicate is significantly favored with sufficient silicate ions. On the other hand, unlike clay, the chemical composition of sludge has a higher contribution of CaO derived from the decomposition of calcite, dolomite and the transformation of francolite to fluorapatite. Therefore the ratio MO/SiO_2 is greater than 1, in this case, the formation of Pyrosilicate was significantly favored. This leads to the crystallization of akermanite phase which is a pyrosilicate (contain $Si_2O_7^{6-}$ ions which are formed by joining two tetrahedral SiO_4^{4-} which share one oxygen atom at one corner). However, The composition reported by a ternary diagram (Fig. 13) indicates that the natural diopside contains higher proportions of SiO_2 and minor proportions of CaO and MgO, which fits with the theoretical composition of metasilicate ($MO/SiO_2 = 1$). From the result above we can conclude that the main crystalline phase changed from akermanite ($Ca_2MgSi_2O_7$) to diopside as the $(CaO + MgO)/SiO_2$ ratio decreased. These results are in accordance with the study of Liu et al. [26].

From the thermodynamic point of view, the temperature of the formation of diopside is lower than that of akermanite, which suggests that diopside is more likely to form [24,25].

The XRD pattern of the mixtures samples after heat treatment at 900 and 1120 °C shows that when the clay content was less than 75 wt%, the main crystalline phase formed in samples was the diopside. However, anorthite started to form with clay contents of more than 75 wt%. With decreasing sludge content, the intensity of anorthite became stronger while that of diopside became weaker. This result indicates that the increase in CaO/SiO_2 ratio seems to reduce the crystallinity of anorthite but favors the formation of diopside. This is in accordance with literature [26,27]. Remarkable change was noticed, including the decrease in quartz peaks in XRD patterns of the mixture, which means it reacted to form diopside phase. The presence of diopside and fluorapatite phases is suitable for the manufacture of glass–ceramic [19–21]. It is claimed that the fluorapatite–diopside glass–ceramic shows a combination of high chemical resistance, good biocompatibility and good mechanical strength. Such materials are used as artificial implants in orthopedic surgery [28–30]. Consequently,

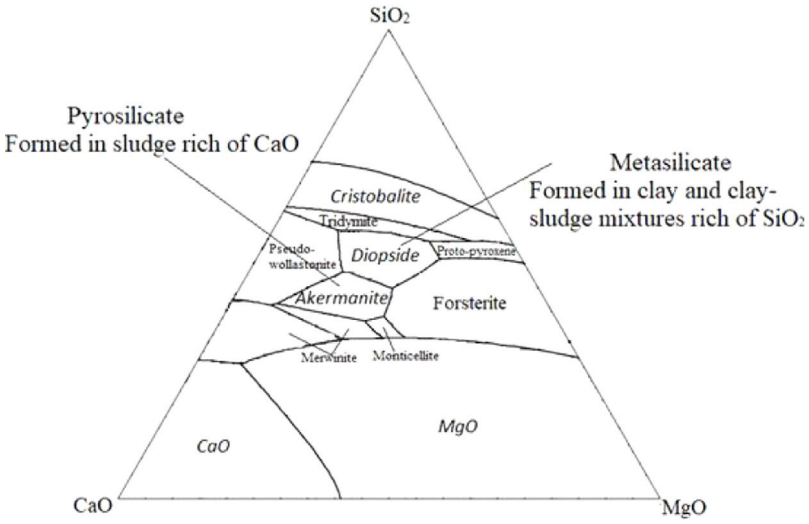

Fig. 13 – Ternary diagram of system SiO_2–CaO–MgO [16,26].

the mixture of phosphate sludge and clay can be used as raw materials in the production of glass–ceramics.

Conclusion

The study focused on the mineralogical and chemical characterization of the phosphate sludge and the study of its thermal behavior alone and when mixed with Safi clay. Based on the results of this investigation, it can be concluded that the phosphate sludge is mainly composed of quartz, calcite, dolomite, and francolite. In contrast, clay samples contained different phases, quartz, illite, kaolinite, dolomite, and calcite.

The presence of quartz, alumina, calcium oxide, and magnesium oxide leads to two new crystalline phases anorthite and akermanite developed respectively in the clay and phosphate sludge samples during the sintering at temperatures ranging from 900 to 1120 °C. The XRD patterns of the mixtures, sintering at 900 °C and 1120 °C, revealed that crystalline diopside and fluorapatite were the most abundant minerals in the mixture contain 50 wt% of sludge, and the formation of metasilicate (diopside) is significantly favored by the addition of sludge.

This study has provided new data on the mineralogical changes that take place in ceramic due to the addition of phosphate sludge. These data will be useful for the manufacturing of high-value-added ceramics. The presence of diopside, fluorapatite phases are suitable for the manufacture of glass–ceramic. The formation of diopside–fluorapatite at high temperature with an important addition of phosphate sludge, pave the way for another study will be focused on the preparation of diopside–fluorapatite based glass–ceramics from phosphate sludge and Safi clay.

REFERENCES

[1] M. Loutou, M. Hajjaji, M. Mansori, C. Favotto, R. Hakkou, Phosphate sludge: thermal transformation and use as lightweight aggregate material, J. Environ. Manage. 130 (2013) 354–360, http://dx.doi.org/10.1016/j.jenvman.2013.09.004.

[2] R. Hakkou, M. Benzaazoua, B. Bussière, Valorization of phosphate waste rocks and sludge from the Moroccan phosphate mines: challenges and perspectives, Procedia Eng. 138 (2016) 110–118, http://dx.doi.org/10.1016/j.proeng.2016.02.068.

[3] O. Ouakibi, S. Loqman, R. Hakkou, M. Benzaazoua, The potential use of phosphatic limestone wastes in the passive treatment of AMD: a laboratory study, Mine Water Environ. 324 (2013) 266–277, http://dx.doi.org/10.1007/s10230-013-0226-8.

[4] R. Hakkou, M. Benzaazoua, B. Bussière, Laboratory evaluation of the use of alkaline phosphate wastes for the control of acidic mine drainage, Mine Water Environ. 28 (2009) 206–218, http://dx.doi.org/10.1007/s10230-009-0081-9.

[5] S. Moukannaa, M. Loutou, M. Benzaazoua, L. Vitola, J. Alami, R. Hakkou, Recycling of phosphate mine tailings for the production of geopolymers, J. Clean. Prod. 185 (2018) 891–903, http://dx.doi.org/10.1016/j.jclepro.2018.03.09.

[6] M. Loutou, M. Hajjaji, A. Babram, M. Mansori, C. Favotto, Phosphate sludge-based ceramics: microstructure and effects of processing factors, J. Build. Eng. (2017), http://dx.doi.org/10.1016/j.jobe.2017.04.002.

[7] M. Loutou, M. Hajjaji, M. Mansori, C. Favotto, R. Hakkou, Heated blends of phosphate waste: microstructure characterization, effects of processing factors and use as a phosphorus source for alfalfa growth, J. Environ. Manage. 177 (2016) 169–176, http://dx.doi.org/10.1016/j.jenvman.2016.04.030.

[8] A. Manni, A. Elhaddar, A. El, I. El Amrani, E. Hassani, C. Sadik, Case studies in construction materials complete characterization of berrechid clays (Morocco) and manufacturing of new ceramic using minimal amounts of feldspars: economic implication, Case Stud. Constr. Mater. 7 (2017) 144–153, http://dx.doi.org/10.1016/j.cscm.2017.07.001.

[9] J.M. Mcarthur, Francolite geochemistry – compositional controls during formation, diagenesis, metamorphism and weathering, Geochim. Cosmochim. Acta 49 (1985) 23–35, http://dx.doi.org/10.1016/0016-7037(85)90188-7.

[10] F. Bolourchifad, A. Memar, The study of phosphate rock forming minerals (frencolite) of Iran through the EDX-SEM to assessment of composition in nano-scale, Procedia Mater. Sci. 11 (2015) 108–111, http://dx.doi.org/10.1016/j.mspro.2015.11.120.

[11] A. Matthews, Y. Nathan, The decarbonation of carbonate–fluorapatite (francolite), Am. Mineral. 62 (1977) 565–573, https://pdfs.semanticscholar.org/51e1/8ed0a8c0071d27ed747371438df7e403ca11.pdf.
[12] Y.T. Algoufi, G. Kabir, B.H. Hameed, Synthesis of glycerol carbonate from biodiesel by-product glycerol over calcined dolomite, J. Taiwan Inst. Chem. Eng. 70 (2017) 179–187, http://dx.doi.org/10.1016/j.jtice.2016.10.039.
[13] S. Mahmoudi, A. Bennour, E. Srasra, F. Zargouni, Characterization, fi ring behavior and ceramic application of clays from the Gabes region in South Tunisia, Appl. Clay Sci. (2016), http://dx.doi.org/10.1016/j.clay.2016.09.023.
[14] A.K. Sharafabadi, M. Abdellahi, A. Kazemi, A. Khandan, N. Ozada, A novel and economical route for synthesizing akermanite ($Ca_2MgSi_2O_7$) nano-bioceramic, Mater. Sci. Eng. C 71 (2017) 1072–1078, http://dx.doi.org/10.1016/j.msec.2016.11.021.
[15] F. Shamoradi, R. Emadi, H. Ghomi, Fabrication of monticellite–akermanite nanocomposite powder for tissue engineering applications, J. Alloys Compd. 693 (2017) 601–605, http://dx.doi.org/10.1016/j.jallcom.2016.09.219.
[16] B. Joachim, E. Garde, R. Abart, W. Heinrich, Akermanite reaction rims between experimental growth of a wollastonite and monticellite: evidence for volume diffusion control, Contrib. Mineral. Petrol. 161 (2011) 389–399, http://dx.doi.org/10.1007/s00410-010-0538-7.
[17] A.C.S. Alcântara, M.S.S. Beltrão, H.A. Oliveira, I.F. Gimenez, L.S. Barreto, Characterization of ceramic tiles prepared from two clays from Sergipe – Brazil, Appl. Clay Sci. 39 (2008) 160–165, http://dx.doi.org/10.1016/j.clay.2007.05.004.
[18] G. Sedmale, I. Sperberga, Formation of high-temperature crystalline phases in ceramic from illite clay and dolomite, J. Eur. Ceram. Soc. 26 (2006) 3351–3355, http://dx.doi.org/10.1016/j.jeurceramsoc.2005.10.012.
[19] M.J. Trindade, M.I. Dias, J. Coroado, F. Rocha, Mineralogical transformations of calcareous rich clays with fi ring: a comparative study between calcite and dolomite rich clays from Algarve, Portugal, Appl. Clay Sci. 42 (2009) 345–355, http://dx.doi.org/10.1016/j.clay.2008.02.008.
[20] D.U. Tulyaganov, S. Agathopoulos, H.R. Fernandes, J.M. Ventura, J.M.F. Ferreira, Preparation and crystallization of glasses in the system tetrasilicic mica–fluorapatite–diopside, J. Eur. Ceram. Soc. 24 (2004) 3521–3528, http://dx.doi.org/10.1016/j.jeurceramsoc.2003.11.026.
[21] L. Zhao, Y. Li, Y. Zhou, D. Cang, Preparation of novel ceramics with high CaO content from steel slag, Mater. Des. 64 (2014) 608–613.
[22] J. Jalali, M. Balghouthi, H. Ezzaouia, Characterization of porous clay ceramics used to remove salt from the saline soils, Appl. Clay Sci. 126 (2016) 259–267, http://dx.doi.org/10.1016/j.clay.2016.03.024.
[23] S. Kurama, E. Ozel, The influence of different CaO source in the production of anorthite, Ceram. Int. 35 (2009) 827–830, http://dx.doi.org/10.1016/j.ceramint.2008.02.024.
[24] P. Hudon, I.H. Jung, D.R. Baker, Experimental investigation and optimization of thermodynamic properties and phase diagrams in the systems $CaO–SiO_2$, $MgO–SiO_2$, $CaMgSi_2O_6–SiO_2$ and $CaMgSi_2O_6–Mg_2SiO_4$ to 1.0 GPa, J. Petrol. 46 (2005) 1859–1880, http://dx.doi.org/10.1093/petrology/egi037.
[25] I. Jung, S.A. Decterov, A.D. Pelton, Critical thermodynamic evaluation and optimization of the $CaO–MgO–SiO_2$ system, J. Eur. Ceram. Soc 25 (2005) 313–333, http://dx.doi.org/10.1016/j.jeurceramsoc.2004.02.012.
[26] H.S.L.Z.B. Liu, Y.B. Zong, H.Y. Ma, W.B. Dai, Effect of $(CaO + MgO)/SiO_2$ ratio on crystallisation and properties of slag glass–ceramics, Adv. Appl. Ceram. 113 (2014) 411–418, http://dx.doi.org/10.1016/j.ceramint.2003.11.005.
[27] Z. Yang, Q. Lin, S. Lu, Y. He, G. Liao, Y. Ke, Effect of CaO/SiO_2 ratio on the preparation and crystallization of glass–ceramics from copper slag, Ceram. Int. 40 (2014) 7297–7305, http://dx.doi.org/10.1016/j.ceramint.2013.12.071.
[28] S.N. Salama, H. Darwish, H.A. Abo-Mosallam, Crystallization and properties of glasses based on diopside–Ca–Tschermak's–fluorapatite system, J. Eur. Ceram. Soc. 25 (2014) 1133–1142, http://dx.doi.org/10.1016/j.jeurceramsoc.2004.04.025.
[29] S.N. Salama, H. Darwish, H.A. Abo-Mosallam, HA forming ability of some glass–ceramics of the $CaMgSi_2O_6–Ca_5(PO_4)_3F–CaAl_2SiO_6$ system, Ceram. Int. 32 (2006) 357–364, http://dx.doi.org/10.1016/j.ceramint.2005.03.012.
[30] J. Chen, B. Yan, H. Li, P. Li, H. Guo, Vitrification of blast furnace slag and fluorite tailings for giving diopside–fluorapatite glass–ceramics, Mater. Lett. 218 (2018) 309–312, http://dx.doi.org/10.1016/j.matlet.2018.02.020.